



This is a repository copy of *Continuous reactive crystallization of pharmaceuticals using impinging jet mixers*.

White Rose Research Online URL for this paper:
<http://eprints.whiterose.ac.uk/112944/>

Version: Accepted Version

Article:

Liu, WJ, Ma, CY, Liu, JJ et al. (2 more authors) (2017) Continuous reactive crystallization of pharmaceuticals using impinging jet mixers. *AIChE Journal*, 63 (3). pp. 967-974. ISSN 0001-1541

<https://doi.org/10.1002/aic.15438>

© 2016 American Institute of Chemical Engineers. This is the peer reviewed version of the following article: Liu, W. J., Ma, C. Y., Liu, J. J., Zhang, Y. and Wang, X. Z. (2017), Continuous reactive crystallization of pharmaceuticals using impinging jet mixers. *AIChE J.*, 63: 967–974. doi: 10.1002/aic.15438, which has been published in final form at <https://doi.org/10.1002/aic.15438>. This article may be used for non-commercial purposes in accordance with Wiley Terms and Conditions for Self-Archiving. Uploaded in accordance with the publisher's self-archiving policy.

Reuse

Unless indicated otherwise, fulltext items are protected by copyright with all rights reserved. The copyright exception in section 29 of the Copyright, Designs and Patents Act 1988 allows the making of a single copy solely for the purpose of non-commercial research or private study within the limits of fair dealing. The publisher or other rights-holder may allow further reproduction and re-use of this version - refer to the White Rose Research Online record for this item. Where records identify the publisher as the copyright holder, users can verify any specific terms of use on the publisher's website.

Takedown

If you consider content in White Rose Research Online to be in breach of UK law, please notify us by emailing eprints@whiterose.ac.uk including the URL of the record and the reason for the withdrawal request.

Continuous Reactive Crystallization of Pharmaceuticals

Using Impinging Jet Mixers

Wen J. Liu¹, Cai Y. Ma¹, Jing J. Liu², Yang Zhang² and Xue Z. Wang^{1,2,*}

¹School of Chemical and Process Engineering, University of Leeds, Leeds LS2 9JT, United Kingdom

²School of Chemistry and Chemical Engineering, South China University of Technology, Guangzhou, China 510640

AUTHOR INFORMATION

Dr. Wen J. Liu (University of Leeds, now works in China University of Petroleum)

Email: 37648984@qq.com

Dr. Cai Y. Ma (University of Leeds)

Email C.Y.Ma@leeds.ac.uk

Dr. Jing J. Liu (South China University of Technology)

Email: cejjliu@scut.edu.cn

Dr. Yang Zhang (South China University of Technology)

Email: ceyzhang@scut.edu.cn

***Corresponding Author:**

Prof Xue Z. Wang

Chair in Intelligent Measurement and Control

Institute of Particle Science and Engineering

School of Chemical and Process Engineering

University of Leeds, Leeds LS2 9JT, UK

Tel +44 113 343 2427, Fax +44 113 343 2384

Email x.z.wang@leeds.ac.uk

ABSTRACT

For reactive crystallization of pharmaceuticals that show rapid reaction rate, low solubility of active pharmaceutical ingredient, hence large supersaturation, it was found in a recent study that a process design that integrates an impinging jet mixer and a batch stirred tank, the former to achieve intensive micromixing prior to reaction and crystal nucleation and the later to immediately disperse the formed nuclei or small particles to minimise aggregation but promote crystal growth, has produced high quality crystals. The current investigation studies the hypothesis that due to the short processing time of reactive crystallization, the impinging jet mixer - stirred tank design can be made to operate in continuous mode. The new design combines an impinging jet mixer for feed introduction and reaction, and a continuous stirred tank reactor (CSTR) and a tubular reactor for crystal growth. Study on reactive crystallization of sodium cefuroxime (an antibiotic), using firstly in a 1L CSTR then scaled to 50L CSTR, found that the new design has produced crystals of higher crystallinity, narrower particle size, and improved product stability, than the conventional batch crystallizer.

KEYWORDS:

Reactive crystallization; continuous crystallization, continuous processing of pharmaceuticals, impinging jet mixer; process analytical technology; sodium cefuroxime

INTRODUCTION

Reactive crystallization of sodium cefuroxime, an antibiotic, showed rapid reaction rate, low solubility of sodium cefuroxime in the solvent, and as a result very large supersaturation¹. Based on this mechanistic understanding, a process design was reported recently¹ that has an impinging jet mixer submerged in the solution of a batch stirred tank crystallizer, with the thinking that the former achieves intensive micromixing of fluids prior to reaction and nucleation and the later disperses immediately the formed nuclei of active pharmaceutical ingredient (API) or the small particles to minimise their aggregation and promote crystal growth. The design showed improved performance than stirred tank crystallizers that were used in industry in the manufacture of an active pharmaceutical ingredient, sodium cefuroxime.

The current study was motivated by the hypothesis that the kind of pharmaceutical reactive crystallization processes similar to the production of sodium cefuroxime is very suited for continuous mode operation. Firstly, the impinging jets for feeding the reactants are already in continuous operational mode in the design of the impinging jet mixer plus stirred batch crystallizer¹. Secondly, the steps involved in the reactive crystallization, from feeding, to contact of reactants, to formation of crystals, are relative rapid processes, completing in minutes, instead of hours. Since the volume of a continuous stirred tank reactor (crystallizer) (CSTR), or the length of a tubular reactor (crystallizer) is often decided by the residence time required in processing the materials, long residence time might mean unrealistic large tank volume or very long tube if continuous mode operation was employed. In fact, the requirement on sufficiently long residence time is one of the major challenges facing when conversing from batch to continuous mode operation in pharmaceutical manufacture processing. Some innovative work has been reported such as the design of continuous oscillatory baffled

crystallizer² in which very slow continuous flow velocity was achieved in a tubular continuous crystallizer as a result of the mixing created by the oscillatory baffles, consequently the use of a short tube was able to achieve long residence time. For the rapid reactive crystallization, due to its short time required, is very suited for continuous operation. Continuous processing of pharmaceuticals has numerous potential advantages such as the avoidance of batch to batch variations and easy to achieve precision control of processes. These potential advantages have prompted the recent research interest world-wide such as the creation of the Novartis-MIT Center on Continuous Manufacturing of Pharmaceuticals³.

There is limited literature on continuous reactive crystallization is mainly for inorganic materials or for standard CSTR or tubular designs^{4-8, 9-14}. Tavaré et al.¹⁵ studied a process involving the elementary chemical reaction between two reactants, subsequent crystallization of the product took place in a continuous crystallizer. Yin et al.^{16,17} researched a reactive precipitation process in a continuous isothermal mixed suspension-mixed product removal crystallizer. Schoenecker et al.¹⁸ implemented a scale-up procedure for producing amine-functionalized UiO-66 which led to the development of a novel flow-through metal-organic framework synthesis process. They scaled up a continuous-flow reactive crystallization process by using a draft-tube type reactor.

In our study, the synthesis of sodium cefuroxime was chosen as a representative organic reactive crystallization process. Sodium cefuroxime is a valuable antibiotic, which has high activity against a wide range of gram-positive and gram-negative micro-organisms.^{19,20} However, its poor stability has been a cause of widespread concern. During storage and transportation, it tends to deepen in colour.^{21,22} In our previous work¹, using process analytical technology (PAT) based on focused beam reflectance measurement (FBRM) and a stirred-tank crystallizer combined with a novel impinging jet mixer design, the synthesis of sodium cefuroxime was optimized and scaled up to 10L successfully.

The stability of the obtained product was improved remarkably with the impinging jet mixer - batch stirred tank configuration¹. Midler et al.²³ described a method using impinging fluid jet streams in a continuous crystallization process to achieve high intensity micromixing of fluids so as to form a homogeneous compound prior to the start of nucleation. The process permits the direct crystallization of particles with high surface area. Lindrud et al.²⁴ and AmEnde et al.²⁵ described an apparatus and process for crystallizing submicron-sized particles with the introduction of a sonic probe with impinging jets. The previous work is inspiring though some design and operational conditions were not given in details. Other recent research on impinging jet crystallization was from Tari et al.²⁶ and Liu et al.¹. Tari et al. studied antisolvent crystallization of glycine and found that it produced small crystals with narrow size distribution. In addition to experimental research, there was also work on modelling of impinging jet crystallizers²⁷.

In the current work, the impinging jet mixer - batch stirred tank configuration¹ is further developed and a continuous mode process design for carrying out reactive pharmaceutical crystallization is presented. The design consists of a pair of impinging jets that continuously feed the reactants, allowing them to intensively mix, react and generate nuclei, a continuous stirred tank reactor (crystallizer) (CSTR) that disperses the nuclei and small particles, and a pipe linked to the CSTR in which crystals undergo further growth in a plug flow pattern. Reactive crystallization producing antibiotic sodium cefuroxime is used as the case study.

In the next section, the materials, the process design, and the instruments used will be firstly introduced. Then in Section three, the chemical reaction, crystal growth, and flow and mixing behavior were analyzed. Section four reports the experimental results obtained in both a 1L CSTR system and a 50L CSTR system.

MATERIALS, PROCESS, AND INSTRUMENTS

Materials

The reactants are cefuroxime acid ($C_{16}H_{16}N_4O_8S$, $424.37 \text{ kg}\cdot\text{mol}^{-1}$, water content $< 0.2\%$) and 60% w/w sodium lactate aqueous solution (Fisher Scientific UK Ltd).²² Ethanol (95% v/v) and activated carbon were obtained from Fisher Scientific UK Ltd, acetone was obtained from Sigma, and the distilled water was produced in our laboratory.

The reaction solutions were prepared by dissolving 9.0 g 60 % w/w sodium lactate aqueous solution in the mixed solvent of 40 mL acetone and 50 mL 95 % ethanol at 20 - 25°C. The mixture was then filtered and washed with 10 mL 95 % ethanol in a beaker. Afterwards 10 g acid cefuroxime was dissolved in the mixed solvent of 246 mL acetone and 124 mL 95 % ethanol. Activated carbon was added in the acid cefuroxime solution and the mixture was stirred for 10 - 15 minutes at 38 - 42°C, then filtered and the activated carbon was washed with 30 mL acetone. Finally, the product, sodium cefuroxime crystals, was filtered and washed in a mixture of acetone and 95% ethanol (1.8 : 1) until the pH value reached 8.0. After 24 hours vacuum drying in a DZF-6030B vacuum oven, the final product was obtained.

The Process

The process layout is shown in Figure 1 (Figure 1 is for 1L CSTR; the 50L CSTR design is different only in dimensions). A pair of impinging jets, as continuous feeding pipes of reactants, is inserted into a CSTR. The jets should be placed as close as possible to the CSTR impeller and be submerged in the solution (slurry). It should be noted that it was also tested to put the jet mixers above the liquid, but the result was found in our early study not as good as submerging them in the solution. Attached to the CSTR is a tube from which the slurries are continuously withdrawn. During an operation, the reactants, cefuroxime acid ($C_{16}H_{16}N_4O_8S$, $424.37 \text{ kg}\cdot\text{mol}^{-1}$, water content $< 0.2\%$) and 60% w/w sodium lactate, are introduced at room temperature by the two jets, and then meet, mix and react at

the jets' ends to form sodium cefuroxime. Since sodium cefuroxime has very low solubility in the solvent, it crystallise to forms nuclei immediately. The nuclei (and small crystals) are immediately dispersed in the solution of the stirred tank by the impeller of the CSTR to avoid immediate rapid aggregation. The slurry stays in the CSTR for a short time, decided by the CSTR volume, before flowing into the tube in which the crystals in the slurry continue to grow and the slurry is withdrawn at the end as the final crystal product.

An alternative design could have been to link the jet mixers directly to a tubular crystallizer, eliminating the CSTR. The main consideration of not removing the CSTR was that since the solubility of sodium cefuroxime is very low, the CSTR stirrer impeller will disperse the nuclei and small particles as soon as they are formed (if, as we did, the impinging jet mixer is placed close to the stirrer impeller), this will prevent possible spontaneous aggregation of the nuclei. Whether this will benefit the crystallization process can be analysed by examining the mechanism of crystal growth in a reactive crystallization process. The mechanism that crystals get bigger in a reactive crystallization process is still under debate, but the dominant view at the moment is that it is a combined process of nuclei (and small crystals) aggregation and surface growth (by absorbing molecules or ions to its surfaces)^{28,29}. Dispersing the nuclei (and small particles) as soon as they are formed in the CSTR near the feeding mixer means the dilution of the nuclei and small particles, which could promote surface growth and slower aggregation in contrast to rapid spontaneous aggregation.

Another possible alternative configuration is to eliminate the tubular part connected to the CSTR. However, the near plug flow condition in the tubular crystallizer often produces crystals with more uniform sizes (narrow crystal size distribution) than in a CSTR. Tubular crystallizers were less commonly used in practice than CSTR tubular crystallizers mainly due to other factors, for example,

crystals could stick to the tube wall causing blockage of the tube. In this study for sodium cefuroxime crystallization, no such difficulties were encountered for the tubular crystallizer.

Instruments

FBRM (LASENTEC, S400A Controller, PI-14/206 PROBE) was used to monitor crystallization processes and also to provide qualitative and quantitative information about nucleation and crystal growth.³⁰⁻³⁴ UV (SHIMADZU UVmini-1240) was used for reaction kinetics determination. X-ray diffraction data was collected using Bruker D8 advance (CuK α 1, $\lambda = 1.540598 \text{ \AA}$). Yttria (Y₂O₃) was used as standard for the estimation of instrumental peak broadening. The crystal size distribution was measured using Morphologi G3 of Malvern Instrument. The Morphologi G3 measures the size and shape of particles using the technique of static image analysis.

STUDY ON THE REACTION, CRYSTAL GROWTH AND FLOW

Characterization of the Reaction

An UV spectrometer was used to study the characteristics of reaction by measuring the concentration of acid cefuroxime. The characteristic absorption peak of acid cefuroxime is around 274 nm.³⁵ In the UV spectrum range, ethanol has no absorption, but acetone has absorption which can cause interference. So a mixed solvent of ethanol and acetone under the same ratio as the reaction solvent was made for UV spectrometer baseline data collection. The solutions of acid cefuroxime (C₁) used for UV spectrometer calibration ranged from 0 mol·L⁻¹ (cefuroxime/solvent) to 0.2 mol·L⁻¹ (step length is 0.02 mol·L⁻¹), which covered the entire change of the reaction concentration. The calibration curve is given in Figure 2, which ~~is~~ almost follows a straight line.

The calibrated UV spectrometer was used to measure the gradually depletion of acid cefuroxime concentration during the reaction. A beaker instead of the sample cell provided by the spectrometer

was used because firstly it was found that as the reaction occurred, the solution in the cell became turbid rapidly due to particles generated that affected UV measurement, and secondly there was no stirrer in the UV spectroscopy sample cell so the reactants could not achieve full mixing. A magnetic stirrer was put into the beaker, and then as soon as the reactants were added into the beaker, the timer started. After every minute, the clear supernatant solution was drawn out by a pipette and put into the spectrometer cell for measurement. When the measurement was completed in about 10 seconds, the solution was put back into the beaker. In this way, the impact of particles was avoided and the measurement process more closely mimics the real reaction operation. Five experiments were conducted and the concentrations were averaged. Figure 3 presented the relationship of the mean concentration values versus the reaction time.

As can be seen in Figures 3 and 4, the reaction reached completion in about 8 minutes, and $\ln(C_{10}/C_1)$ versus reaction time was a straight line, indicating that the reaction is most likely first-order. It needs to point out that the reaction time in the impinging jet mixer - CSTR could be slightly shorter than 8 minutes because of the improved mixing. Nevertheless, the UV measured reaction time provides useful information about the reaction.

Characterization of Crystal Growth

Several theories exist to explain the mechanisms of crystal growth.³⁶ The diffusion-reaction theory suggests that once an ordered crystal structure is formed by nucleation, the growth units (atoms, ions or molecules) can diffuse from the surrounding supersaturated solution to the surface of the nucleus and resulting in crystal growth. Adsorption layer theory suggests that particle growth happens on pre-exist layers of atoms or molecules that adsorbed on crystals faces. For rapid reactive crystallization it was thought that in addition surface growth, aggregation of small particles including nuclei is another factor causing crystal size growth.^{37,38,28,39}

FBRM was used here for characterization of crystal growth. The result is given in Figure 5. It was observed that the total counts (an indicative measure of number of crystals) of crystals of all size ranges continuously increased for about 15 minutes, then the counts in the size range of 1 μm - 5 μm started to drop first, and the total counts of particles started to drop almost at the same time. Then counts in the ranges of 10 μm - 23 μm and 29 μm - 86 μm also dropped, leaving only the counts of the largest particles ($> 100 \mu\text{m}$) still kept increasing. Figure 5 also indicated that at about 25th minute crystals no longer grow in size.

In the above, the reaction and crystal growth behaviour has been studied. Thermodynamic data is available from our previous study,²² so it will not be repeated here.

CFD simulation of the mixing and flow behaviour

Computational fluid dynamics (CFD) analysis using the ANSYS Fluent 13 software was made to study the 1L tank reactor with the impinging jet mixers and tubular reactor. Figure 6 shows that the CFD computational domain. Sliding mesh was used in the mixing paddle region of the stirred tank reactor. The setting of interface was also used to achieve the mass and heat transfer between the mixing paddle region and the main reactor region. The entire reactor was compartmentalized by three-dimensional mesh with 255269 tetrahedral cells in total where the main reactor region contains 228142 cells and the mixing paddle region has 27127 cells. Since the diameters of the feeding nozzles and the outlet tube were much smaller than the reactor diameter, the surface mesh construction was used firstly to ensure the uniformity of the grid, and then using grid's own amplifying function, the whole mesh was generated automatically. Grid-independent and step-independent were verified before simulation.

Pure single-phase flow simulation was carried out firstly and compared with the previous experimental data. The properties of single-phase liquid material used in the simulation were the same as the solvent mixture (ethanol and acetone) used in the experiment. Parameter settings including reaction temperature, feed rate and stirring speed were based on the values obtained from the experiments.¹ Standard SIMPLE pressure-velocity coupling was used with a first-order upwind scheme being employed for the discretization of the convection terms in the governing equations. Due to the insulation of the system, heat losses through the outer wall of the reactor were assumed to be negligible. Standard non-slip wall boundary conditions were applied in the studies with the standard turbulent wall function being used. Since the reaction is neither endothermic nor exothermic, the temperature of the entire reactor was set constant. The material properties of the solvent such as density, viscosity, thermal conductivity and specific heat were also set to fixed values.³⁰

The cases simulated here were the impact of the nozzles' angles on the flow state. From Figure 7, the following observations can be made: (a) for 10° upward nozzles, the high-speed zone in the middle of the two nozzles indicated that it could guarantee the two reactants frontal mid-way collision. However, after collision, the rapid decline of the velocity indicated that it was difficult for the mixture to leave the mixing zone (impinging jet mixer region) into the tank reactor; (b) for the parallel nozzles the high-speed zone moved to one side obviously, indicating that the nozzles could guarantee the two reactants colliding in the mid-way, and the collision speed was relative lower than the other two cases, and the mixing effect might not be satisfactory. This result explained why in experiments the parallel nozzles had led to crystal accumulation which caused clogging of the nozzle;¹ and (c) for 10° downward nozzles, the advantages of the former two cases were reflected: the two reactants were able to collide in the mid-way with high speed and the mixture could flow into the tank reactor without problem.

To make the simulation as close as possible to the real process, the Eulerian-Eulerian two-phase flow simulation approach was then applied for estimating the residence time and residence time distribution, which means particles were added into the crystallizer in simulation. The properties of these particles were taken as the same as sodium cefuroxime. Species transport equation was used and the other settings remained the same with single-phase flow simulation. Residence time distribution (RTD) was simulated because it can be used to compare with two ideal reactor models, ideal plug flow reactor and mixed flow reactor. In an ideal plug-flow reactor, there is no axial mixing and the fluid elements leave in the same order as they arrived. Therefore, the variance σ^2 of an ideal plug-flow reactor is zero. In mixed flow reactors, an ideal continuous stirred-tank reactor is based on the assumption that the flow at the inlet is completely and instantly mixed into the bulk of the reactor. The reactor and the outlet fluid have identical, homogeneous compositions at all times. Therefore, the variance of an ideal mixed-flow reactor σ^2 is one.⁴⁰ The RTD of a real reactor deviate from that of an ideal reactor, depending on the hydrodynamics within the vessel.

To estimate the residence time distribution of the tank reactor via CFD simulation, a small amount of inert substance fluid was injected into the ~~novel~~ reactor from the impinging jet probe and the concentration change of the inert substance was modelled at the outlet of the reactor (0 mm in Figure 6). The concentration was normalized first, and then the function $E(t)$ was obtained. As can be seen in Figure 8(a), in all cases the residence time was no less than 8 minutes. It was also observed that mixing effects of the three nozzle designs were significantly different. The variance σ^2 results indicated that the 10° downward nozzles provide the best mixing followed by the parallel, and the 10° upward was the worst. This conclusion was also consistent with the pure single-phase flow simulation results, which further illustrated the importance of mixing for reaction processes. The variance σ^2 results also indicated that the design that adding impinging jets and the stirrer into the reactor made this tank reactor closer to an ~~the~~ ideal mixed flow reactor.

For estimating the RTD in the tubular reactor, a little amount of inert substance fluid was injected into the reactor from 0 mm in Figure 6 and the concentration change of this inert substance was monitored at different lengths (1500mm, 1700mm, 2000 mm, and 2500 mm in Figure 6). As can be seen in Figure 8(b), in all cases the residence time in the tubular reactor was no less than 22 minutes. As analysed earlier, the reaction and crystal growth came to completion in about 25 minutes. The residence time in the chosen CSTR and that in the tubular reactor add together to give about 30 minutes, larger than the required 25 minutes for the completion of reaction and crystal growth. So the sizes of the selected CSTR and tubular reactor are suitable.

EXPERIMENTAL RESULTS AND DISCUSSION

Experiments in the 1L Crystallizer

The 1L system is as sketched in Figure 1. The reaction temperature (controlled by a Julabo circulator) was 25 - 28°C. The stirring speed (controlled by an IKA EUROSTAR digital stirrer) was kept at around 80 rpm. The velocity of introducing feed via the impinging jet mixer was 10 m·s⁻¹ (controlled by 307 Piston Pumps).

Tube lengths of 1500 mm, 1700mm and 2000mm were used for the tubular part. Figure 9 shows the peak intensities of products obtained for the three lengths (other parts of the system and operational conditions were the same), indicating that 1700mm and 2000mm lengths give similar XRD patterns, slightly better than 1500 mm. The particle mean size and size distribution of the products under these two lengths were also very close. As a result, a tube length of 1700 mm was chosen for conducting four repeated experiments (20130626, 20130627, 20130628, and 20130701), which produced the same good quality products (their XRD results are shown in Figure 10). From the stability test results, as shown in Table 1, it can be seen that the products obtained from this new process design was more stable (improved about three colour grades) compared with conventional batch crystallizers.

Experiments in the 50L Crystallizer

For the 50L crystallizer, the design of the impinging jets was the same as in the 1L crystallizer: 10° downward and 6.78 mm spacing. The reactant feed velocity in the impinging mixers was also the same as in the 1L system, i.e. 10 m/s, and stirring speed 80 rpm. The length of the tubular part was 5 m with the diameter being 5.6 cm.

The XRD spectra for crystals obtained from the 50L system were given in Figure 11, showing almost identical patterns as crystals produced from the 1L crystallizer. It can also be seen from the Morphologi G3 results in Figure 12, the crystal size distribution of products obtained from the 50L system were much better than the products obtained from the conventional batch crystallizer. The mean size was smaller with no bimodal phenomenon. As can be seen from the stability results (Table 2), the colour grade of products of the 50L system were almost the same as the products from the 1L design, higher than the products obtained from the conventional batch crystallizer by three colour grades under 60°C accelerated stability tests.

CONCLUSIONS

The process consisting of a mixer of impinging jets and a CSTR followed by a tubular reactor was designed and tested for reactive crystallization of an antibiotic, sodium cefuroxime, mainly for the purpose of improving the drug's stability. The design was based on the idea that the impinging jet mixer creates intensive mixing for reactants and for nucleation; the nuclei and small particles were immediately dispersed in the CSTR to avoid immediate intensive aggregation, then the mixture flows into the tubular reactor to allow crystals to grow (via the combined mechanisms of crystal growth: face growth and aggregation). For the tested pharmaceutical, no blockage or other operational difficulties were experienced. The experiments were carried out on both a 1L CSTR system and a 5L CSTR system. Both cases demonstrated similar performance. The sodium cefuroxime crystals

showed significantly improved stability during 60⁰C accelerated stability tests in comparison with crystals obtained from conventional batch crystallizers.

ACKNOWLEDGMENTS

Financial Support from UK Engineering and Physical Sciences Research Council (EP/H008012/1, EP/H008853/1), China Scholarship Council (CSC), and funding of the China Thousand Talents Scheme, the National Natural Science Foundation of China (NNSFC) under its Major Research Scheme of Meso-scale Mechanism and Control in Multi-phase Reaction Processes (project reference: 91434126), as well as Natural Science Foundation of Guangdong Province (project title: Scale-up study of protein crystallization based on modelling and experiments) are gratefully acknowledged.

REFERENCES

1. Liu WJ, Ma CY, Liu JJ, Zhang Y, Wang XZ. Analytical Technology Aided Optimization and Scale-Up of Impinging Jet Mixer for Reactive Crystallization Process. *AIChE Journal*. 2015; 61:503-517.
2. Lawton S, Steele G, Shering P, Zhao L, Laird I, Ni X-W. Continuous Crystallization of Pharmaceuticals Using a Continuous Oscillatory Baffled Crystallizer. *Organic Process Research & Development*. 2009; 13:1357-1363.
3. Novartis-MIT Centre for Continuous Manufacturing, <https://novartis-mit.mit.edu/>. accessed, February 2015.
4. Kitamura M, Konno H, Yasui A, Masuoka H. Controlling factors and mechanism of reactive crystallization of calcium carbonate polymorphs from calcium hydroxide suspensions. *Journal of Crystal Growth*. 2002; 236:323-332.
5. Kotaki Y, Tsuge H. Reactive crystallization of calcium-carbonate in a batch crystallizer. *Journal of Crystal Growth*. 1990; 99:1092-1097.
6. Tsuge H, Kotaki Y, Hibino S. Reactive crystallization of calcium-carbonate by liquid-liquid reaction. *Journal of Chemical Engineering of Japan*. 1987; 20:374-379.
7. Tsuge H, Okada K, Yano T, Fukushi N, Akita H. Reactive crystallization of magnesium hydroxide. In: Botsaris G, Toyokura K, eds. *Separation and Purification by Crystallization*. Vol 6671997:254-266.
8. Tsuge H, Yoshizawa S, Tsuzuki M. Reactive crystallization of calcium phosphate. *Chemical Engineering Research & Design*. 1996; 74:797-802.

9. Kozik A, Matynia A. Continuous reaction crystallization of struvite under stoichiometric conditions. *Przemysl Chemiczny*. 2012; 91:823-827.
10. Koralewska J, Hutnik N, Piotrowski K, Wierzbowska B, Matynia A. Effect of reactive crystallization parameters on the quality of struvite crystals produced in a continuous draft tube magma crystallizer with a jet pump fed with recirculated mother solution. *Przemysl Chemiczny*. 2009; 88:472-476.
11. Loan M, Newman OGM, Farrow JB, Parkinson GM. Effect of rate of crystallization on the continuous reactive crystallization of nanoscale 6-line ferrihydrite. *Crystal Growth & Design*. 2008; 8:1384-1389.
12. Cole KP. Continuous amide bond formation and reactive crystallization. *Abstracts of Papers of the American Chemical Society*. 2013; 246.
13. Hutnik N, Wierzbowska B, Matynia A. Continuous reactive crystallization of struvite from a solution containing phosphate(V) and potassium ions. *Przemysl Chemiczny*. 2013; 92:791-795.
14. Quon JL, Zhang H, Alvarez A, Evans J, Myerson AS, Trout BL. Continuous Crystallization of Aliskiren Hemifumarate. *Crystal Growth & Design*. 2012; 12:3036-3044.
15. Tavare NS. Mixing, reaction and precipitation: An interplay in continuous crystallizers. *Chemical Engineering Science*. 1994; 49:5193-5201.
16. Yin QX, Wang JK, Xu Z, Li GZ. Analysis of concentration multiplicity patterns of continuous isothermal mixed suspension-mixed product removal reactive precipitators. *Industrial & Engineering Chemistry Research*. 2000; 39:1437-1442.
17. Yin QX, Wang JK, Zhang M, YL. W. Influence of nucleation mechanisms on the multiplicity patterns of agglomeration-controlled crystallization. *Industrial & Engineering Chemistry Research*. 2001; 40:6221-6227. *Industrial & Engineering Chemistry Research*. 2001; 40:6221-6227.
18. Schoenecker P, Belancik G, Grabicka B, Walton K. Kinetics study and crystallization process design for scale-up of UiO-66-NH₂ Synthesis. *Aiche Journal*. 2013; 59:1255-1262.
19. Gower P, Dash C. Pharmacokinetics of cefuroxime after intravenous-injection. *European Journal of Clinical Pharmacology*. 1977; 12:221-227.
20. Greenwood D, Pearson N, O'Grady F. Cefuroxime a new cephalosporin antibiotic with enhanced stability to enterobacterial beta lactamases. *Journal of Antimicrobial Chemotherapy*. 1976; 2:337-343.
21. Fu G, Zhou Z, Dong Q, Long W, Inventors. Preparation of cefuroxime sodium. US patent CN 101906109 A. Dec 8, 2010.
22. Liu WJ, Ma CY, Feng SX, Wang XZ. Solubility measurement and stability study of sodium cefuroxime. *Journal of Chemical & Engineering Data*. 2014; 59:807-816.
23. Midler M, Paul EL, Whittington EF, Futran M, Liu PD, Hsu J, Pan S-H, Inventors. Crystallization method to improve crystal structure and size. US patent U.S. 5,314,5061994.

24. Lindrud MD, Kim S, Wei C, Inventors. Sonic impinging jet crystallization apparatus and process. US patent US 6,302,958 B1. US 6,302,958 B1, 2001.
25. AmEnde D, Crawford T, Weston N, Inventors. Reactive crystallization method to improve particle size. US 6,558,435 B2, 2003.
26. Tari T, Fekete Z, Szabó-Révész P, Aigner Z. Reduction of glycine particle size by impinging jet crystallization. *International Journal of Pharmaceutics*. 2015; 478:96-102.
27. Woo XY, Tan RBH, Braatz RD. Modeling and computational fluid dynamics-population balance equation-micromixing simulation of impinging jet crystallizers. *Crystal Growth & Design*. 2009; 9:156-164.
28. Chen M, Ma CY, Mahmud T, Darr JA, Wang XZ. Modelling and simulation of continuous hydrothermal flow synthesis process for nano-materials manufacture. *Journal of Supercritical Fluids*. 2011; 59:131-139.
29. Erriguible A, Mariasi F, Cansell F, Aymonier C. Monodisperse model to predict the growth of inorganic nanostructured particles in supercritical fluids through a coalescence and aggregation mechanism. *Journal of Supercritical Fluids*. 2009; 48:79-84.
30. Barrett P, Glennon B. In-line FBRM monitoring of particle size in dilute agitated suspensions. *Particle & Particle Systems Characterization*. 1999; 16:207-211.
31. Heath AR, Fawell PD, Bahri PA, Swift JD. Estimating average particle size by focused beam reflectance measurement (FBRM). *Particle & Particle Systems Characterization*. 2002; 19:84-95.
32. Saleemi AN, Rielly CD, Nagy ZK. Comparative investigation of supersaturation and automated direct nucleation control of crystal size distributions using ATR-UV/vis spectroscopy and FBRM. *Crystal Growth & Design*. 2012; 12:1792-1807.
33. Saleemi AN, Rielly CD, Nagy ZK. Monitoring of the combined cooling and antisolvent crystallisation of mixtures of aminobenzoic acid isomers using ATR-UV/vis spectroscopy and FBRM. *Chemical Engineering Science*. 2012; 77:122-129.
34. Doki N, Yokota M, Sasaki S, Kubota N. Simultaneous crystallization of D- and L-asparagines in the presence of a tailor-made additive by natural cooling combined with pulse heating. *Crystal Growth & Design*. 2004; 4:1359-1363.
35. Wozniak TJ, Hicks JR. Analytical profile of cefuroxime sodium. *Analytical profiles of drug substances*. 1991; 20:209-236.
36. Kossel W. The energetics of surface procedures. *Annalen Der Physik*. 1934; 21:457-480.
37. Lu J, Wang JK. Agglomeration, breakage, population balance, and crystallization kinetics of reactive precipitation process. *Chemical Engineering Communications*. 2006; 193:891-902.
38. Morgan N, Wells C, Kraft M, Wagner W. Modelling nanoparticle dynamics: coagulation, sintering, particle inception and surface growth. *Combustion Theory and Modelling*. 2005; 9:449-461.

39. Ma CY, Chen M, Wang XZ. Modelling and simulation of counter-current and confined-jet reactors for hydrothermal synthesis of nano-materials. *Chemical Engineering Science* 2014; 109:26-37.
40. Wood T. A note concerning residence time distribution in a cylindrical vessel. *Chemical Engineering Science*. 1962; 17:391-392.

Table 1.Stability Test Data of Sodium Cefuroxime Obtained from the 1L Experiments*

Batch No.	60°C					
	0 day	5 days	7 days	10 days	14 days	20 days
Original	<Y-2	<Y-5	<Y-7	<Y-9	<Y-9	<Y-10
20130626	<Y-2	<Y-3	<Y-5	<Y-6	<Y-6	<Y-7
20130627	<Y-2	<Y-3	<Y-4	<Y-5	<Y-6	<Y-7
20130628	<Y-2	<Y-3	<Y-4	<Y-5	<Y-6	<Y-7
20130701	<Y-2	<Y-3	<Y-5	<Y-6	<Y-6	<Y-7

*Y means the colour grade yellow.

Table 2.Stability Test Data of Sodium Cefuroxime Obtained from the 50L Experiments.*

Batch No.	60°C					
	0 day	5 days	7 days	10 days	14 days	20 days
Original	<Y-2	<Y-5	<Y-7	<Y-9	<Y-9	<Y-10
20131020-1	<Y-2	<Y-3	<Y-4	<Y-6	<Y-6	<Y-7
20131020-2	<Y-2	<Y-3	<Y-5	<Y-5	<Y-6	<Y-7
20131021-1	<Y-2	<Y-3	<Y-4	<Y-5	<Y-6	<Y-7
20131021-2	<Y-2	<Y-2	<Y-4	<Y-5	<Y-6	<Y-7

*Y means the colour grade yellow.

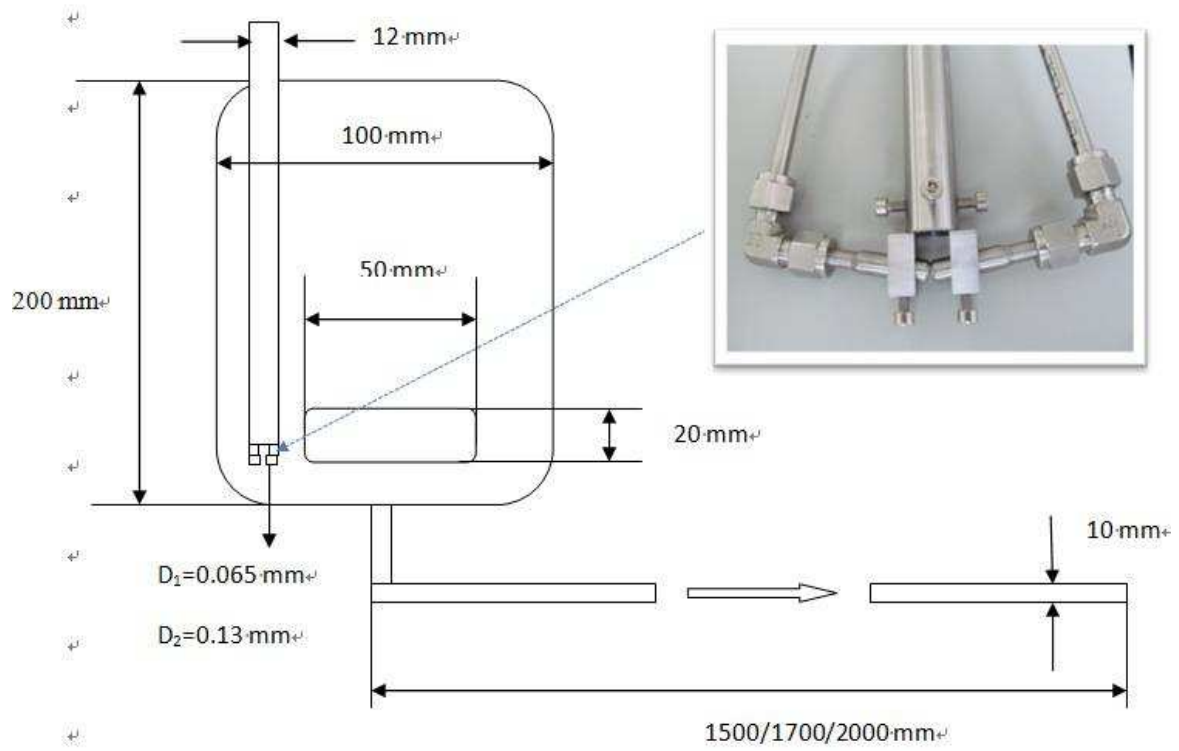


Figure 1. Sketch of the 1L novel crystallizer for sodium cefuroxime reactive crystallization.

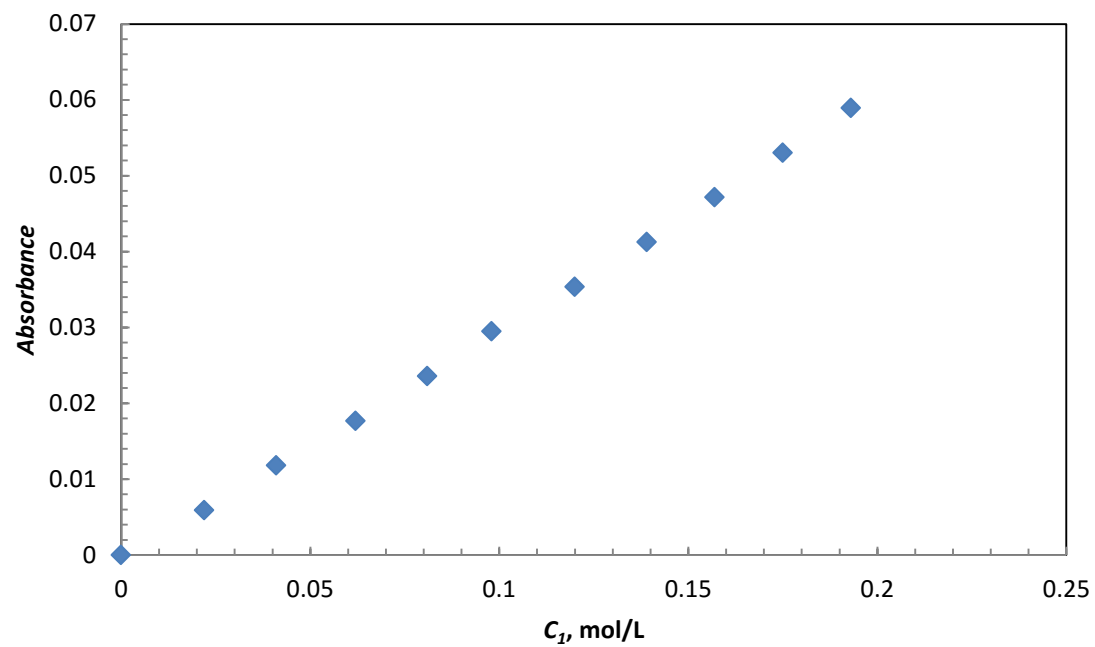


Figure 2. UV spectrometer calibration curve for acid cefuroxime (C₁) from 0 mol·L⁻¹ to 0.2 mol·L⁻¹.

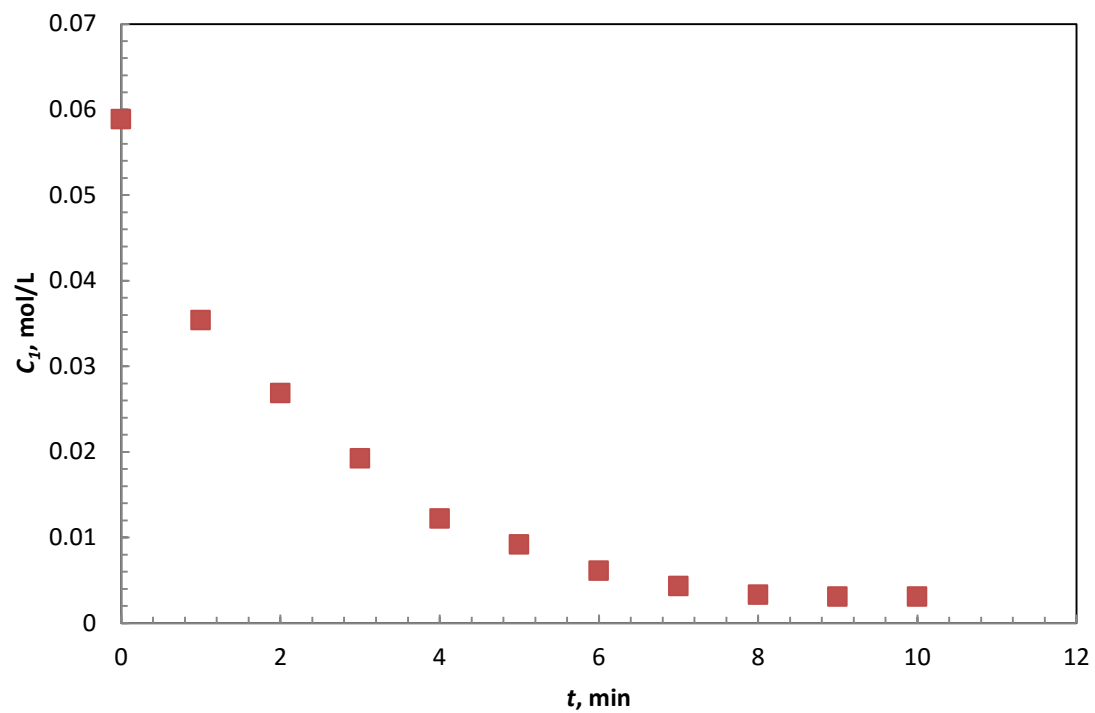


Figure 3. Mean concentration curve of acid cefuroxime (C_1) during the reactive crystallization process measured by ultraviolet–visible spectrometer.

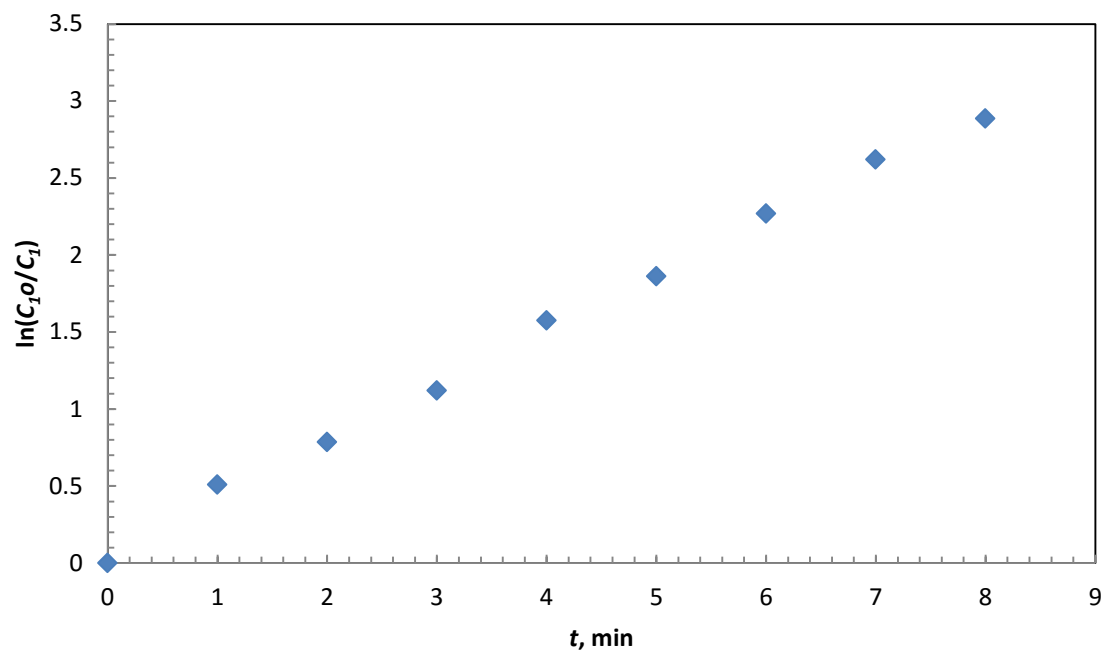


Figure 4. Relative concentration ($\ln (C_{10}/C_1)$) curve of acid cefuroxime (C_1) during the reactive crystallization process measured by ultraviolet–visible spectrometer.

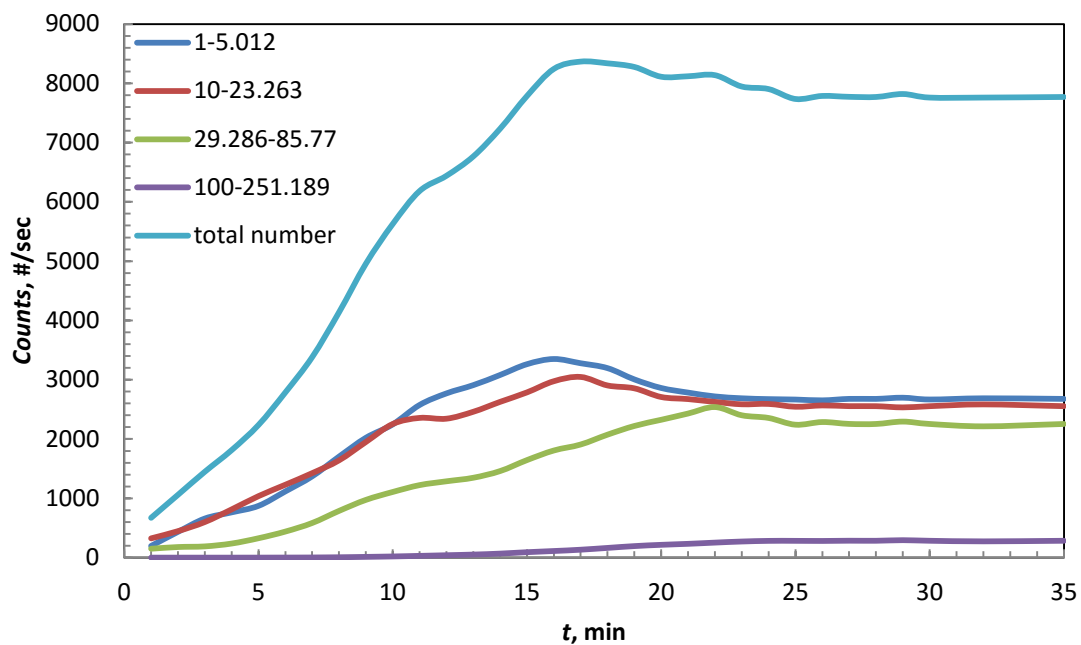


Figure 5. Counts of sodium cefuroxime crystals during the reactive crystallization measured by focused beam reflectance measurement (FBRM).

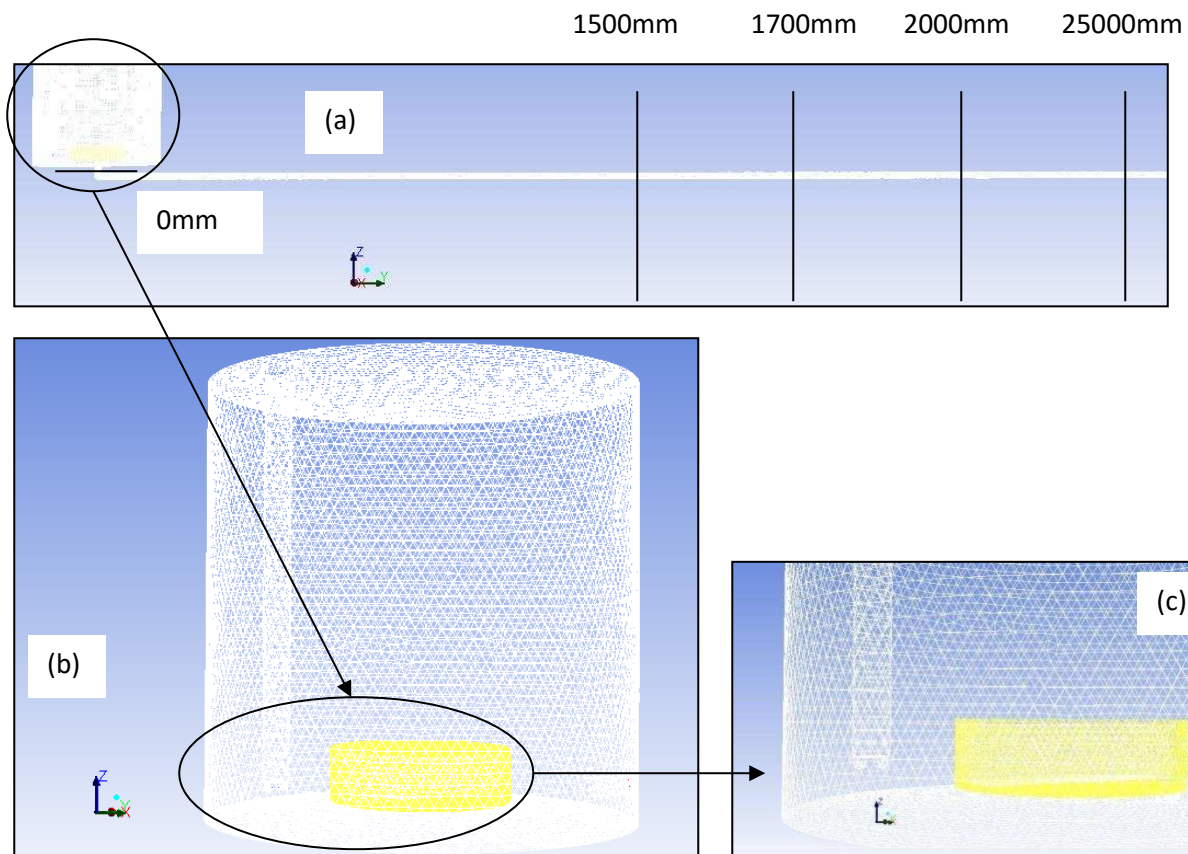


Figure 6. Illustration of the computational mesh of the crystallizer for CFD simulation: (a) overall three-dimensional mesh in reactor region with the collection surface of residence time distribution; (b) mesh in tank reactor with impinging jet mixer probe; and (c) mesh in mixing paddle region.

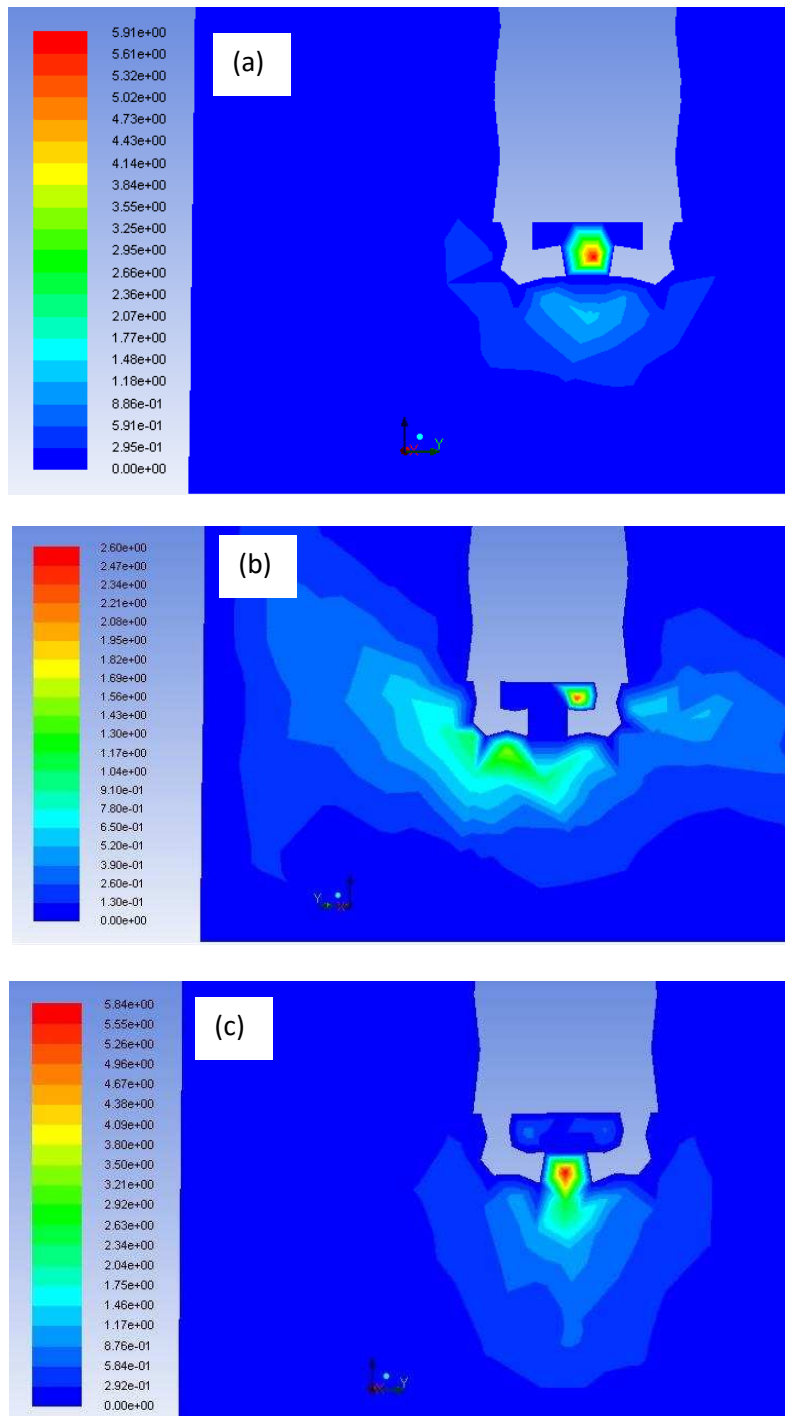


Figure 7. Velocity distribution ($\text{m}\cdot\text{s}^{-1}$) in the impinging jet mixer region simulated by CFD single-phase flow: (a) 10° upward nozzles, (b) parallel, and (c) 10° downward.

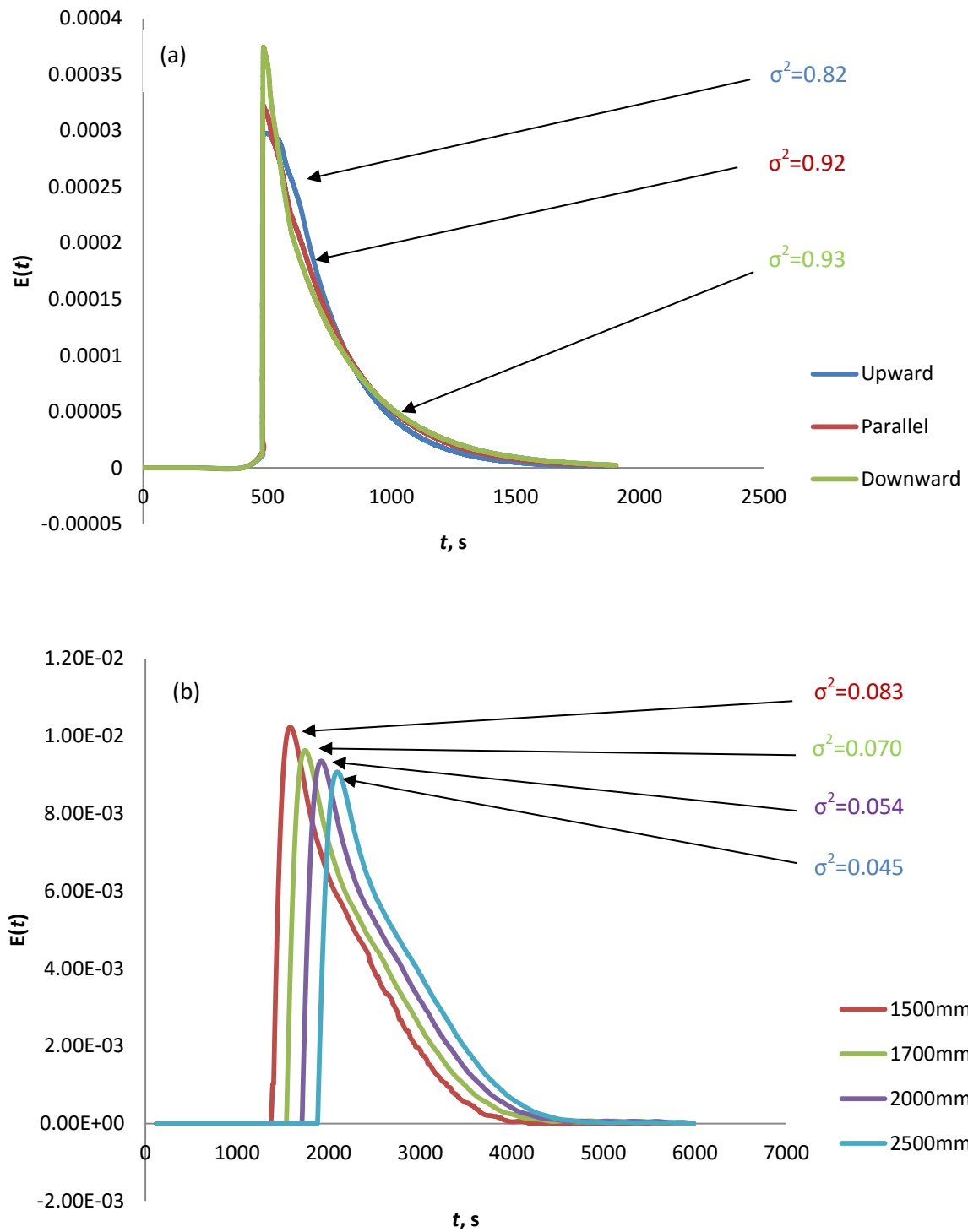


Figure 8. Residence time distribution estimated by CFD Eulerian-Eulerian two-phase flow simulation approach for (a) the CSTR reactor and (b) the tubular reactor.

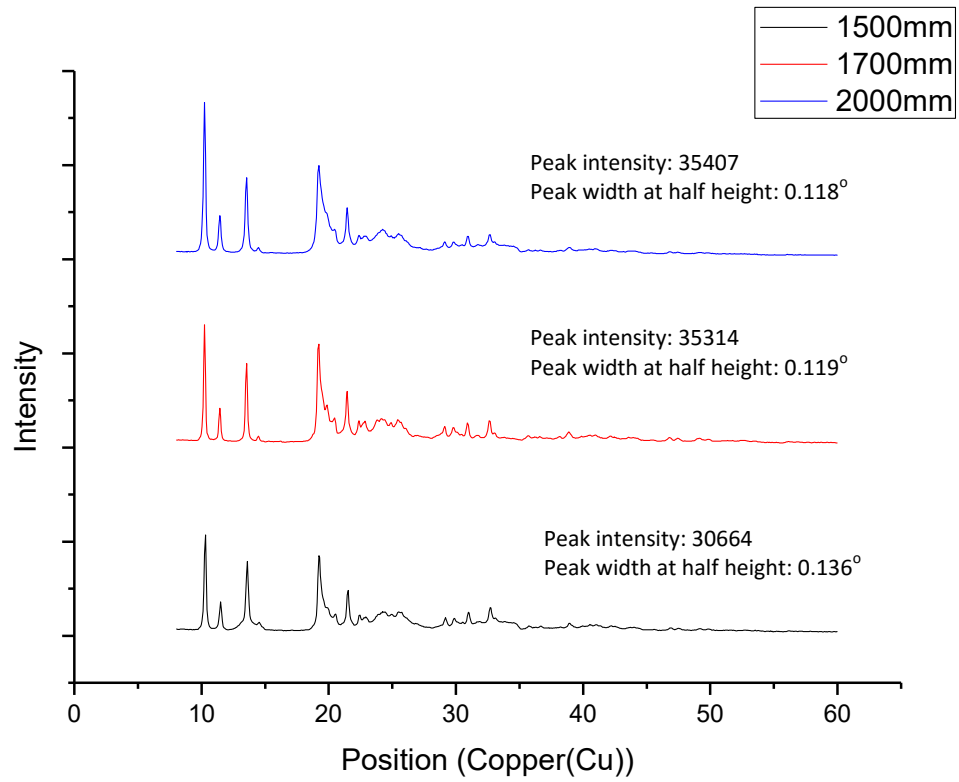


Figure 9. XRD patterns of sodium cefuroxime crystals obtained from 1L experiments (peak intensity and peak width at half height of peak between 9° to 10.5° were chosen to present the crystallinity).

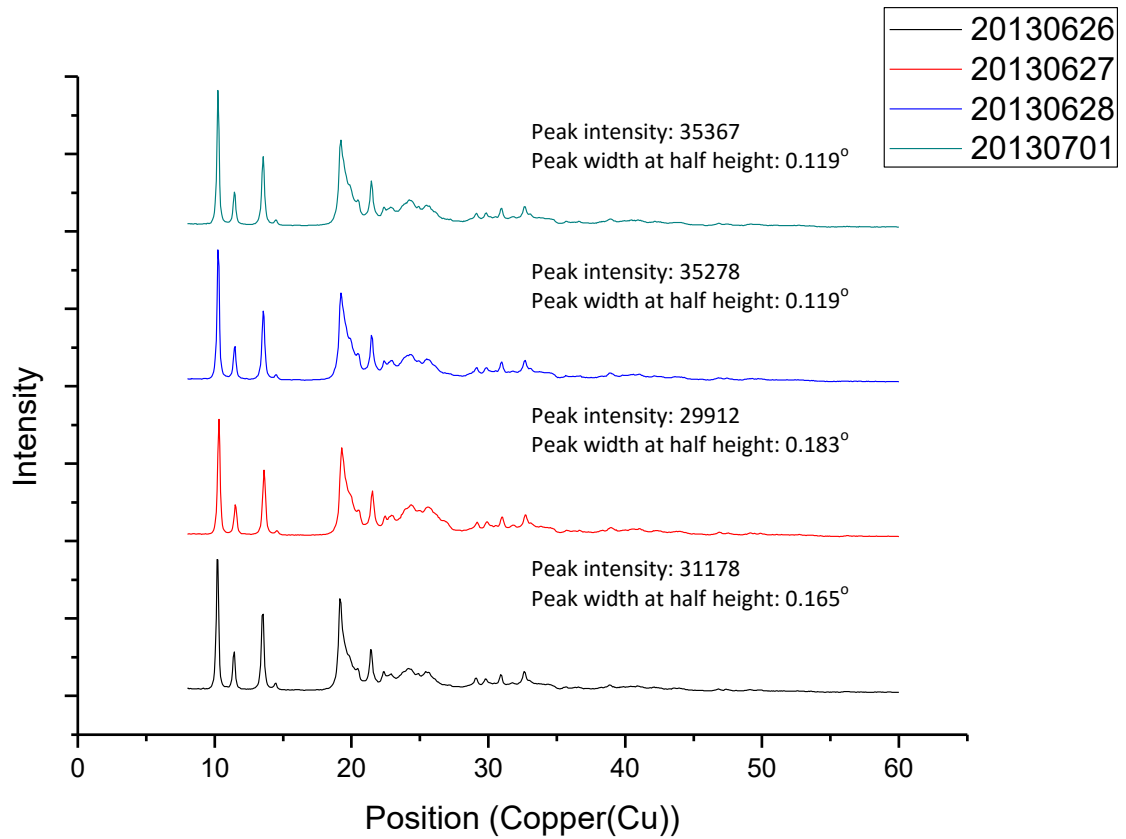


Figure 10. XRD patterns of sodium cefuroxime crystals obtained from 1L four repeated experiments (peak intensity and peak width at half height of peak between 9° to 10.5° were chosen to present the crystallinity).

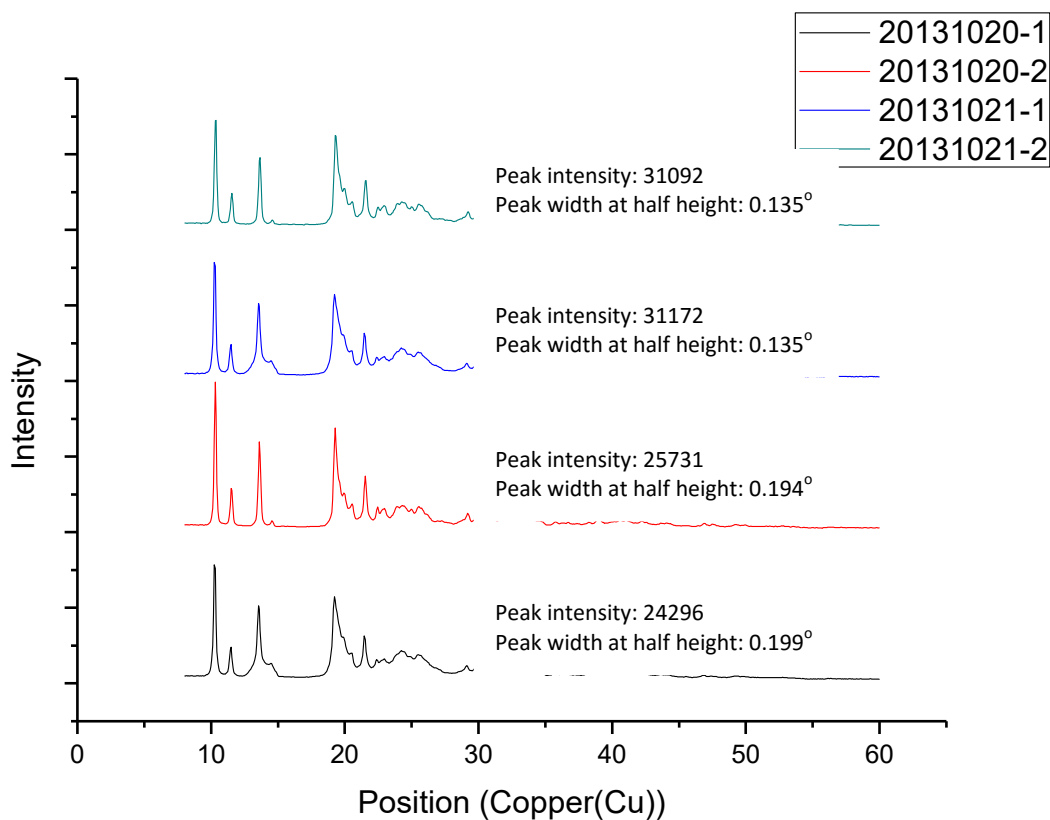


Figure 11. XRD patterns of sodium cefuroxime crystals obtained from 50L scale-up experiments (peak intensity and peak width at half height of peak between 9° to 10.5° were chosen to present the crystallinity).

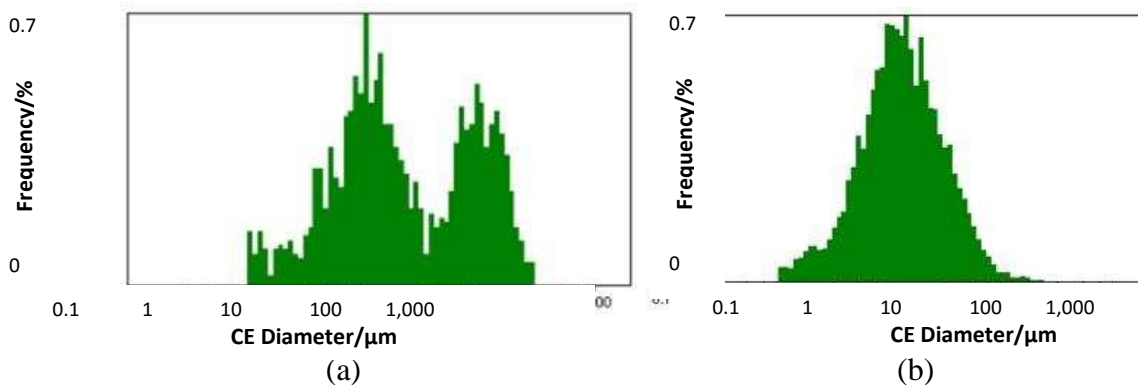


Figure 12. Particle size distribution, analysed by Morphologi G3, for sodium cefuroxime crystals obtained from 50L scale-up experiments: (a) Product obtained from the conventional batch crystallizer; (b) product obtained from the new 50 L continuous crystallizer.